

Ab initio phonon dispersions of Fe and Ni

Andrea Dal Corso and Stefano de Gironcoli
 SISSA, Via Beirut 2/4, 34014 Trieste and INFN Trieste, Italy
 (Received 1 February 2000)

We present the *ab initio* phonon dispersions of magnetic bcc Fe and fcc Ni. Our calculations are carried out in the framework of density functional perturbation theory (DFPT), using ultrasoft pseudopotentials, spin-polarized generalized gradient approximations, and nonlinear core corrections. The implementation of the above techniques within DFPT is discussed. We find that these approximations, together, provide phonon dispersions which are in good agreement with experiment, while the local spin density approximation systematically overestimates the experimental frequencies.

The lattice dynamics of magnetic transition metals is essential in many applications and *ab initio* calculations of their phonon dispersions could provide insight into long-standing problems. For instance, the extremely low thermal expansion coefficient of Invar, a Fe-Ni alloy,¹ could depend on an unusual behavior of the phonon frequencies upon volume changes.

The structural and dynamical properties of magnetic transition metals are determined by the interplay between magnetic and electronic effects which are well described by spin-polarized density functional theory (DFT).² The local spin density approximation (LSDA) for the exchange and correlation energy is sufficient to reproduce the magnetic moments of transition metals.³ However, this approximation sometimes fails to predict their ground-state crystal structure. In Fe, for instance, one must include spin-polarized generalized gradient corrections (σ -GGA) to get the lowest energy for the experimental bcc Bravais lattice.^{4,5} State-of-the-art electronic structure codes provide readily the equilibrium properties of transition metals, and the phonon dispersions can be calculated either with density functional perturbation theory^{6,7} (DFPT) or with frozen phonon techniques, relaxing large supercells. The latter route has been followed in Ref. 8 to compute the phonon dispersion of Fe, while in this paper we present the lattice dynamics of Fe and Ni calculated with DFPT. The advantages of this technique have been stressed in several papers,^{6,9} and therefore it is important to generalize it to magnetic transition metals.

We describe Fe and Ni atoms with ultrasoft pseudopotentials,¹⁰ and freeze the $3s$ and $3p$ electrons in the core, accounting for the nonlinear interaction between the core and the valence charge.¹¹ In Ref. 7, DFPT was generalized to ultrasoft pseudopotentials, and in Ref. 12 the spin-unpolarized GGA has been included in DFPT and applied to Si, C, Al, and Cu. In this paper we discuss DFPT with σ -GGA and with nonlinear core corrections (NLCCs): we analyze the variation of the self-consistent exchange and correlation potential due to a general perturbation, and describe the effect of the spin and of the GGA on the part of the interatomic force constants due to NLCCs. A detailed derivation of the whole theory at this general level will be given elsewhere.¹³ We find that the σ -GGA, with ultrasoft pseudopotentials and NLCCs, predicts accurately the phonon dispersions of both Fe and Ni. In contrast, the LSDA overestimates the phonon frequencies in both elements.

In the σ -GGA, the exchange and correlation energy is a functional of the spin-up and spin-down charge densities [$n_{\uparrow}(\mathbf{r})$ and $n_{\downarrow}(\mathbf{r})$].¹⁴ Thanks to the spin-scaling relation, the exchange energy is the sum of two spin (σ) contributions: $E_x = \sum_{\sigma} \int d^3r G_x(n_{\sigma}, |\nabla n_{\sigma}|)$. Instead, the correlation energy is written as a functional of the total charge $n(\mathbf{r}) = n_{\uparrow}(\mathbf{r}) + n_{\downarrow}(\mathbf{r})$, of its gradient, and of the local spin polarization $\zeta(\mathbf{r}) = [n_{\uparrow}(\mathbf{r}) - n_{\downarrow}(\mathbf{r})]/n(\mathbf{r})$: $E_c = \int d^3r G_c(n, \zeta, |\nabla n|)$. There are several functional forms of G_x and G_c available in the literature, and our theory comprises any exchange and correlation functional for which G_x and G_c can be defined. NLCCs are introduced in this scheme, taking as the spin-up and spin-down charge densities $n_{\sigma}(\mathbf{r})$ the sum of the valence [$\rho_{\sigma}(\mathbf{r})$] and the core charge [$\rho_{c,\sigma}(\mathbf{r})$]: $n_{\sigma}(\mathbf{r}) = \rho_{\sigma}(\mathbf{r}) + \rho_{c,\sigma}(\mathbf{r})$. Core spin polarization is neglected, assuming that $\rho_{c,\sigma}(\mathbf{r}) = \frac{1}{2}\rho_c(\mathbf{r})$, where $\rho_c(\mathbf{r})$ is the total core charge calculated together with the pseudopotential in the neutral, spin-unpolarized, isolated atom.

The exchange and correlation potential has two components, one acting on the spin-up and the other on the spin-down wave functions. These components are evaluated as functional derivatives of the exchange and correlation energy with respect to the spin-up and spin-down charges:

$$\begin{aligned} V_{xc}^{\sigma}(\mathbf{r}) &= \frac{\partial G}{\partial n_{\sigma}} - \sum_{\alpha=1}^3 \frac{\partial}{\partial r_{\alpha}} \left[\frac{\partial G}{\partial (\partial_{\alpha} n_{\sigma})} \right] \\ &= \frac{\partial G_x}{\partial n_{\sigma}} + \frac{\partial G_c}{\partial n} + \frac{\partial G_c}{\partial \zeta} \frac{\partial \zeta}{\partial n_{\sigma}} \\ &\quad - \sum_{\alpha=1}^3 \frac{\partial}{\partial r_{\alpha}} [A_x(n_{\sigma}, |\nabla n_{\sigma}|) \partial_{\alpha} n_{\sigma} \\ &\quad + A_c(n, \zeta, |\nabla n|) \partial_{\alpha} n], \end{aligned} \quad (1)$$

where $G = \sum_{\sigma} G_x + G_c$, $\partial \zeta / \partial n_{\uparrow} = (1 - \zeta)/n$, $\partial \zeta / \partial n_{\downarrow} = -(1 + \zeta)/n$, and the two functions A_x and A_c are defined as

$$A_x(n_{\sigma}, |\nabla n_{\sigma}|) = \frac{1}{|\nabla n_{\sigma}|} \frac{\partial G_x}{\partial |\nabla n_{\sigma}|}, \quad (2)$$

$$A_c(n, \zeta, |\nabla n|) = \frac{1}{|\nabla n|} \frac{\partial G_c}{\partial |\nabla n|}. \quad (3)$$

In a plane-wave implementation, it is numerically convenient to calculate Eq. (1) as it is, without taking explicitly the \mathbf{r} derivatives of $A_x \partial_\alpha n_\sigma + A_c \partial_\alpha n$, but computing these derivatives numerically with Fourier techniques. In this way, V_{xc}^σ is the functional derivative of the exchange and correlation energy even at finite cut offs.¹⁵

Within DFPT, the calculation of the dynamical matrix of a solid requires first-order changes of the wave functions due to phonon perturbations. These quantities are solutions of a

self-consistent linear system. In order to set up this system, the change of the exchange and correlation potential (ΔV_{xc}^σ) must be calculated. This quantity is modified by the introduction of the σ -GGA in the theory. At linear order, ΔV_{xc}^σ is proportional to the induced charge density Δn_σ and to its \mathbf{r} derivatives. Since the correlation energy depends on the total charge and on its gradient, the change of one spin component of the charge modifies both spin components V_{xc}^σ . We have

$$\begin{aligned} \Delta V_{xc}^\sigma(\mathbf{r}) = & \sum_{\sigma'} \left[\frac{\partial^2 G_x}{\partial^2 n_\sigma} \delta_{\sigma\sigma'} + \frac{\partial B_c^\sigma}{\partial n} + \frac{\partial B_c^\sigma}{\partial \zeta} \frac{\partial \zeta}{\partial n_{\sigma'}} \right] \Delta n_{\sigma'} + \sum_{\sigma' \sigma''} \left[\frac{\partial A_x}{\partial n_\sigma} \delta_{\sigma\sigma'} \delta_{\sigma\sigma''} + \frac{1}{|\nabla n|} \frac{\partial B_c^\sigma}{\partial |\nabla n|} \right] \sum_{\beta=1}^3 \partial_\beta n_{\sigma'} \partial_\beta \Delta n_{\sigma''} \\ & - \sum_{\alpha=1}^3 \frac{\partial}{\partial r_\alpha} \left[\sum_{\sigma' \sigma''} \left(\frac{\partial A_x}{\partial n_\sigma} \delta_{\sigma\sigma'} \delta_{\sigma\sigma''} + \frac{1}{|\nabla n|} \frac{\partial B_c^\sigma}{\partial |\nabla n|} \right) \Delta n_{\sigma'} \partial_\alpha n_{\sigma''} + \sum_{\sigma' \sigma'' \sigma'''} \left(\frac{1}{|\nabla n_\sigma|} \frac{\partial A_x}{\partial |\nabla n_\sigma|} \delta_{\sigma\sigma'} \delta_{\sigma\sigma''} \delta_{\sigma\sigma'''} \right. \right. \\ & \left. \left. + \frac{1}{|\nabla n|} \frac{\partial A_c}{\partial |\nabla n|} \right) \sum_{\beta=1}^3 \partial_\beta n_{\sigma'} \partial_\beta \Delta n_{\sigma''} \partial_\alpha n_{\sigma'''} + \sum_{\sigma'} (A_x \delta_{\sigma\sigma'} + A_c) \partial_\alpha \Delta n_{\sigma'} \right], \end{aligned} \quad (4)$$

where B_c^σ are defined as

$$B_c^\sigma = \frac{\partial G_c}{\partial n} + \frac{\partial G_c}{\partial \zeta} \frac{\partial \zeta}{\partial n_\sigma}, \quad (5)$$

and we used the relationships

$$\Delta |\nabla n_\sigma| = \frac{1}{|\nabla n_\sigma|} \sum_{\beta=1}^3 \partial_\beta n_\sigma \partial_\beta \Delta n_\sigma, \quad (6)$$

$$\Delta |\nabla n| = \frac{1}{|\nabla n|} \sum_{\sigma' \sigma''} \sum_{\beta=1}^3 \partial_\beta n_{\sigma'} \partial_\beta \Delta n_{\sigma''}. \quad (7)$$

Again Eq. (4) is the correct functional derivative even at finite cutoffs. Within the LSDA, G_x and G_c do not depend upon the density gradient. Thus only the first term in Eq. (4) is nonvanishing and one recognizes the LSDA expression of $f_{xc}^{\sigma, \sigma'}$ (the functional derivative of the exchange and correlation potential with respect to the charge). As in Ref. 12, we compute analytically G_x, G_c, A_x, A_c , and B_c^σ and numerically their derivatives with respect to $n_\sigma, n, \zeta, |\nabla n_\sigma|$, and $|\nabla n|$. The gradient of Δn_σ is instead evaluated via Fourier techniques.

The introduction of the σ -GGA has no effect on the formal expressions of the second derivatives of the total energy given in Ref. 7 provided that ΔV_{xc}^σ are computed using Eq. (4) and a sum over spin components is done in each term. NLCCs yield two additional contributions as shown in Ref. 16 for the norm-conserving, spin-unpolarized case. In our case, with the notations of Ref. 7 we have

$$\begin{aligned} \Phi_{s,s'} = & \Phi_{s,s'}^{(0)} + \sum_{\sigma} \int d^3 r_1 \Delta^{u_s} V_{xc}^\sigma(\mathbf{r}_1) \frac{d\rho_{c,\sigma}(\mathbf{r}_1)}{d\mathbf{u}_s} \\ & + \sum_{\sigma} \int d^3 r_1 V_{xc}^\sigma(\mathbf{r}_1) \frac{d^2 \rho_{c,\sigma}(\mathbf{r}_1)}{d\mathbf{u}_s d\mathbf{u}_s}. \end{aligned} \quad (8)$$

where $\Phi_{s,s'}^{(0)}$ are the interatomic force constants of Ref. 7. When the local density approximation is used, one recovers in Eq. (8) the NLCC terms given in Ref. 16 by averaging over spins and by separating $\Delta^{u_s} V_{xc}^\sigma$ into a valence and a core contribution: $\Delta^{u_s} V_{xc}^\sigma(\mathbf{r}) = \sum_{\sigma'} f_{xc}^{\sigma, \sigma'}(\mathbf{r}) (\Delta^{u_s} \rho_{\sigma'} + d\rho_{c,\sigma'} / d\mathbf{u}_s)$.

Ultrasoft pseudopotentials¹⁰ for Fe and Ni have been generated according to a modified Rappe-Rabe-Kaxiras-Joannopoulos (RRKJ) scheme¹⁷ with three Bessel functions, following the method of Ref. 18. Relativistic effects are included in the pseudopotentials by solving the Koelling-Harmon scalar relativistic equation¹⁹ to calculate the all-electron reference atomic configuration. Our numerical results are obtained using the Perdew-Burke-Ernzerhof²⁰ (PBE) expressions of G_x and G_c . All GGAs calculations have been performed with pseudopotentials generated consistently within the PBE scheme.²¹ A kinetic energy cutoff of 25 Ry is used for both Fe and Ni. The augmentation charges are expanded up to 400 Ry. This large cutoff for the augmentation charges is needed to minimize the errors in the linear response calculations with the σ -GGA. For the Brillouin zone (BZ) integration we use 240 (bcc) and 60 (fcc) \mathbf{k} points in the irreducible BZ. Integration up to the Fermi surface is done with the smearing technique of Ref. 22 with the smearing parameter $\sigma=0.01$ Ry (Fe) and $\sigma=0.03$ Ry (Ni). These parameters are sufficient to provide phonon frequencies converged within 3 cm^{-1} . The dynamical matrices have

TABLE I. Calculated lattice constants (a_0), bulk modulus (B_0), magnetic moment (μ_0), and cohesive energy (E_c) of bcc Fe and fcc Ni. The atomic energy is obtained at the magnetic ground state ($d^5s^1d^{1.2}s^{0.8}$ for Fe and $d^5s^1d^4s^0$ for Ni). Experimental data are taken from Ref. 24.

	a_0 (a.u.)	B_0 (Mbar)	μ_0 (μ_B)	E_c (eV/atom)
bcc-Fe				
LDSA	5.22	2.33	2.10	6.64
σ -GGA	5.41	1.50	2.38	5.15
Expt.	5.42	1.68	2.22	4.28
fcc-Ni				
LDSA	6.48	2.53	0.59	6.08
σ -GGA	6.65	1.91	0.64	4.88
Expt.	6.65	1.86	0.61	4.44

been computed on a $4 \times 4 \times 4$ \mathbf{q} -point mesh, and a Fourier interpolation has been used to obtain complete phonon dispersions.

We focus on magnetic bcc Fe and magnetic fcc Ni which are the experimental zero-temperature crystal structures. In Table I, we report the equilibrium lattice constants, bulk moduli, and cohesive energies of Fe and Ni obtained from a fit with the Murnaghan equation for the total energy as a function of volume. In the same table we report also the magnetic moment (μ_0) calculated at the theoretical equilibrium lattice constant. (The values of μ_0 have been computed on a mesh of 408 \mathbf{k} points with $\sigma=0.01$ Ry in Ni.) Results obtained using both the LSDA (Ref. 23) and σ -GGA are reported. The experimental lattice constants of Fe and Ni are equal (within the theoretical precision) to the σ -GGA values, and 3.7% (Fe) and 2.6% (Ni) higher than the LSDA values. Our theoretical parameters are in very good agreement with the results of Ref. 24 where pseudopotentials similar to ours have been used. All phonon calculations are performed at the theoretical lattice constants reported in Table I.

The calculated PBE phonon dispersions of magnetic bcc Fe are shown in Fig. 1 along the main high-symmetry lines of the BZ of the bcc lattice and compared with experimental inelastic neutron scattering data. If thermal effects are neglected, very good agreement is found between theory and experiment. The average difference, computed as in Ref. 12, is 6 cm^{-1} and the maximum error (20 cm^{-1}) is found for the

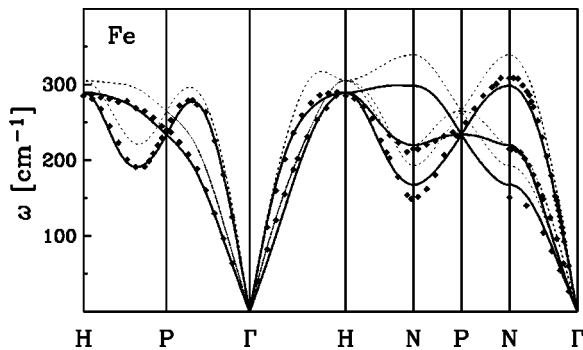


FIG. 1. Calculated σ -GGA phonon dispersions (solid lines) for magnetic bcc Fe compared to inelastic neutron scattering data (solid diamond) and to calculated LSDA dispersions (dotted lines).

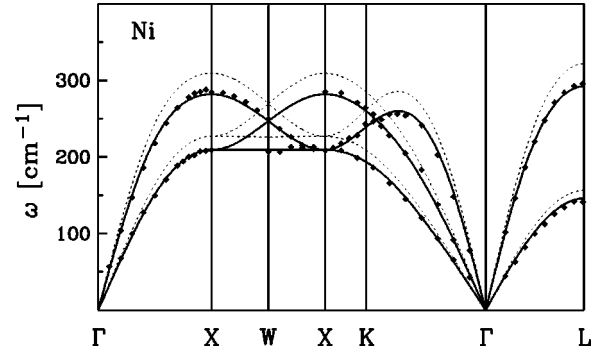


FIG. 2. Calculated PBE phonon dispersions (solid lines) for magnetic fcc Ni compared to inelastic neutron scattering data (solid diamond) and to calculated LSDA dispersions (dotted lines).

transverse acoustic branch along the Γ - H direction. The reported experimental inelastic neutron scattering data are taken at $T=295$ K.²⁵ Temperature and zero-point motion are not included in our calculation. In order to estimate the magnitude of these effects, we have used the experimental thermal expansion coefficient²⁶ and the method of Ref. 27, respectively. From $T=0$ K to $T=295$ K the lattice constant increases by about 0.2%. Furthermore, to account for zero point motion we have to augment the theoretical lattice constant by 0.14%. The PBE phonon frequencies calculated at N with an expanded lattice constant $a_0=5.43$ a.u. are 7 cm^{-1} (T_1), 1 cm^{-1} (T_2), and 13 cm^{-1} (L) lower than the values plotted in Fig. 1. Therefore, taking into account thermal effects, we find that, in Fe, the GGA tends to slightly underestimate the phonon frequencies as in Si, C, and Cu.¹² However, the phonon spectra calculated using the LSDA (Fig. 1) show severe discrepancies with respect to experiment. The average error is 18 cm^{-1} with a maximum error of 44 cm^{-1} along the H - N direction.

The σ -GGA phonon dispersions of Fe, computed along the N - Γ , Γ - H , and H - Γ directions, have been presented also in Ref. 8. These authors used the all-electron projector augmented-wave method²⁸ to deal with Fe. Overall the agreement between the two calculations is good. For instance, the frequency of the T_1 mode at the N point is overestimated by about 22 cm^{-1} in Ref. 8 and 18 cm^{-1} in our calculation.

The calculated PBE phonon dispersions of magnetic fcc Ni are shown in Fig. 2 along the main high-symmetry lines of the BZ of the fcc lattice, and compared with inelastic neutron scattering experimental data. Neglecting thermal effects, excellent agreement is found between theory and experiment. The average error is of 2 cm^{-1} with a maximum error of 11 cm^{-1} for a single point on the T_2 branch along Γ - K . The reported experimental inelastic neutron scattering data are taken at $T=296$ K.²⁹ At this temperature, thermal expansion and zero-point motions, estimated as in Fe, lead to an increase of the lattice constant of about $0.23+0.15=0.38\%$. The PBE phonon frequencies at the X point of the BZ computed with $a_0=6.675$ a.u. are 4 cm^{-1} (TA) and 6 cm^{-1} (LA) lower than the values plotted in Fig. 2. Therefore thermal effects on phonon dispersions are small in Ni and the σ -GGA provides accurate phonon frequencies. In Fig. 2 we display also the LSDA theoretical results. The LSDA turns out to overbind, and the phonon frequencies are correspond-

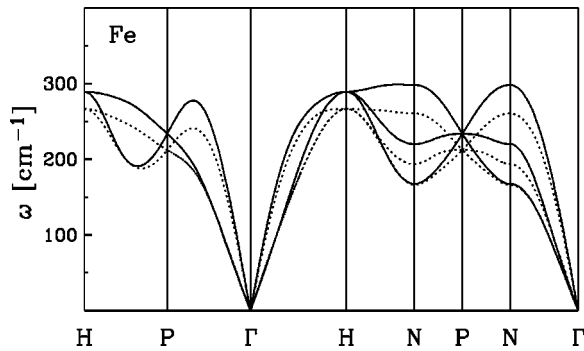


FIG. 3. Calculated PBE (solid lines) and LSDA (dotted lines) phonon dispersions for magnetic bcc Fe, both computed at the experimental lattice constant.

ingly too high. The average error of theory with respect to experiment becomes 15 cm^{-1} with a maximum error of 29 cm^{-1} .

We have estimated the effect of magnetism on the phonon frequencies of Ni by doing one calculation with the spin-unpolarized GGA. The magnetic effects turn out to be quite small. Spin-unpolarized GGA frequencies are, on average, higher of about 3 cm^{-1} with respect to the σ -GGA ones. In Ni, different exchange and correlation functionals, LSDA versus σ -GGA, produce effects much larger than magnetism. On the contrary, in Fe, a proper account of magnetic effects is mandatory, since nonmagnetic bcc Fe is unstable.³⁰

In Figs. 3 and 4, we compare the σ -GGA and LSDA phonon dispersions of Fe and Ni calculated at the experimental lattice constant in order to quantify the effect of the σ -GGA lattice expansion on the final result. The σ -GGA frequencies are stiffer than the LSDA ones when computed at the same lattice constant. The average differences are 17

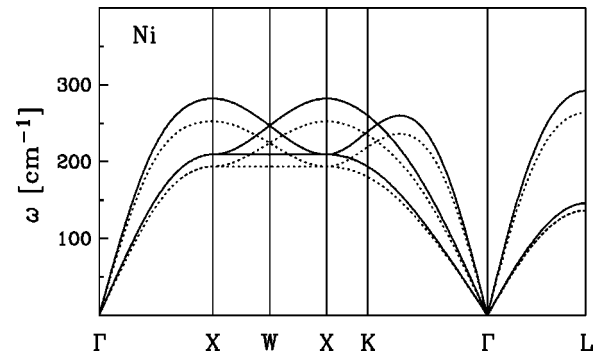


FIG. 4. Calculated PBE (solid lines) and LSDA (dotted lines) phonon dispersions for magnetic fcc Ni, both computed at the experimental lattice constant.

cm^{-1} in Fe and 15 cm^{-1} in Ni. These results are similar to those found in Al and Cu in the spin-unpolarized case.¹²

To conclude we have found that phonon dispersions in Fe and Ni are very well reproduced by the combined use of the GGA, spin polarization, ultrasoft pseudopotentials, and NLCCs. LSDA phonon dispersions are systematically higher than experimental data. Consistently with previous GGA phonon calculations it is found that gradient corrections, added to the LSDA, act as a negative pressure which enlarges the lattice constant and softens the phonon frequencies. In the case of Fe and Ni, this softening brings theory and experiment into much better agreement.

This work has been supported by INFN/F, INFN/G, INFN ‘‘Iniziativa trasversale calcolo parallelo,’’ and MURST (Cofin99). All calculations have been performed with the PWSCF and PHONON codes, to which spin polarization, the σ -GGA, and NLCCs have been added.

¹M. van Schilfhaarde, I.A. Abrikosov, and B. Johansson, *Nature* (London) **400**, 46 (1999).

²S. Lundquist and N. H. March, *Theory of the Inhomogeneous Electron Gas* (Plenum Press, New York, 1983).

³C.S. Wang, B.M. Klein, and H. Krakauer, *Phys. Rev. Lett.* **54**, 1852 (1985).

⁴P. Bagno, O. Jepsen, and O. Gunnarson, *Phys. Rev. B* **40**, 1997 (1989).

⁵D.J. Singh, W.E. Pickett, and H. Krakauer, *Phys. Rev. B* **43**, 11 628 (1991).

⁶S. Baroni, P. Giannozzi, and A. Testa, *Phys. Rev. Lett.* **58**, 1861 (1987); P. Giannozzi, S. de Gironcoli, P. Pavone, and S. Baroni, *Phys. Rev. B* **43**, 7231 (1991); S. de Gironcoli, *ibid.* **51**, 6773 (1995).

⁷A. Dal Corso, A. Pasquarello, and A. Baldereschi, *Phys. Rev. B* **56**, R11 369 (1997).

⁸D. Alfè, G. Kresse, and M.J. Gillan, *Phys. Rev. B* **61**, 132 (2000).

⁹X. Gonze and C. Lee, *Phys. Rev. B* **55**, 10 355 (1997).

¹⁰D. Vanderbilt, *Phys. Rev. B* **41**, 7892 (1990).

¹¹S.G. Louie, S. Froyen, and M.L. Cohen, *Phys. Rev. B* **26**, 1738 (1982).

¹²F. Favot and A. Dal Corso, *Phys. Rev. B* **60**, 11 427 (1999).

¹³A. Dal Corso (unpublished).

¹⁴R.O. Jones and O. Gunnarson, *Rev. Mod. Phys.* **61**, 689 (1989).

¹⁵J.A. White and D.M. Bird, *Phys. Rev. B* **50**, 4954 (1994).

¹⁶A. Dal Corso, S. Baroni, R. Resta, and S. de Gironcoli, *Phys. Rev. B* **47**, 3588 (1993).

¹⁷A.M. Rappe, K.M. Rabe, E. Kaxiras, and J.D. Joannopoulos, *Phys. Rev. B* **41**, 1227 (1990).

¹⁸G. Kresse and J. Hafner, *J. Phys.: Condens. Matter* **6**, 8245 (1994).

¹⁹D.D. Koelling and B.N. Harmon, *J. Phys. C* **10**, 3107 (1977).

²⁰J.P. Perdew, K. Burke, and M. Ernzerhof, *Phys. Rev. Lett.* **77**, 3865 (1996).

²¹We used as reference the all-electron configuration $3d^7 4s^1$ for Fe and $3d^9 4s^1$ for Ni. The core radii (in a.u.) of our pseudopotentials are Fe $4s$ (2.0, 2.2), $4p$ (2.2, 2.3), and $3d$ (1.6, 2.2). The all-electron potential pseudized before $r_c=1.7$ has been taken as a local potential: Ni $4s$ (2.0, 2.5), $4p$ (2.4, 2.6), and $3d$ (1.6, 2.5). The all-electron potential pseudized before $r_c=1.7$ has been taken as a local potential. Two values of the core radii indicate a channel which has been pseudized with the ultrasoft scheme. In such a case, the first value is the norm-conserving core radius and the second is the ultrasoft one.

²²M. Methfessel and A.T. Paxton, *Phys. Rev. B* **40**, 3616 (1989).

²³J. Perdew and A. Zunger, *Phys. Rev. B* **23**, 5048 (1981).

- ²⁴E.G. Moroni, G. Kresse, J. Hafner, and J. Furthmüller, Phys. Rev. B **56**, 15 629 (1997).
- ²⁵B.N. Brockhouse, H.E. Abou-Helal, and E.D. Hallman, Solid State Commun. **5**, 211 (1967).
- ²⁶*American Institute of Physics Handbook*, 3rd ed., edited by D. E. Gray *et al.* (McGraw-Hill Book, New York, 1972), p. 4-125 (Fe), 4-126 (Ni).
- ²⁷P.B. Allen, Philos. Mag. B **70**, 527 (1994).
- ²⁸P.E. Blöchl, Phys. Rev. B **50**, 17 953 (1994); G. Kresse and D. Joubert, *ibid.* **59**, 1758 (1999).
- ²⁹R.J. Birgeneau, J. Cordes, G. Dolling, and A.D.B. Woods, Phys. Rev. **136**, A1359 (1964).
- ³⁰H.C. Herper, E. Hoffmann, and P. Entel, Phys. Rev. B **60**, 3839 (1999).